

**Inhomogeneous superconducting state of superconducting networks in a magnetic field**

Osamu Sato\*

*Department of Liberal Arts, Osaka Prefectural College of Technology, Neyagawa, Osaka 572-8572, Japan*Masaru Kato<sup>†</sup>*Department of Mathematical Sciences, Osaka Prefecture University, 1-1 Gakuencho, Sakai, Osaka 599-8531, Japan  
and CREST, JST, 4-1-8, Honcho, Kawaguchi, Saitama 332-0012, Japan*

(Received 19 March 2003; published 16 September 2003)

Making use of de Gennes–Alexander’s network equation, we have investigated the transition temperature of superconducting honeycomb and square lattice networks in magnetic field. We found that the decrease of the transition temperature  $T_C$  of the finite cluster due to the external field is small compared with that of the periodic networks. At  $T \lesssim T_C$ , the superconducting order parameter becomes inhomogeneous for the finite clusters with edge in contrast to the case of the infinite lattice with periodic boundary condition. Also we obtained the distribution of quantized fluxoids from the winding number of the phase of the order parameter.

DOI: 10.1103/PhysRevB.68.094509

PACS number(s): 74.20.De, 74.81.Fa, 74.25.Qt

**I. INTRODUCTION**

Multiply connected superconductors show peculiar responses to the external magnetic field. A simple example is the Little-Parks experiment,<sup>1,2</sup> which shows periodic variation of the phase-transition temperature as a function of the magnetic field. The period is called a matching field, which is  $\Phi_0$  divided by the area of the hole. Here  $\Phi_0 = hc/2e$  is the flux quantum for superconductivity.

Superconducting networks are extreme examples of multiply connected superconductors. They consist of superconducting thin wires, which are connected to each other regularly or randomly. In the limit where we can ignore the width of the wires, superconducting order parameter may be considered as uniform across the cross section of the wires.

Recently, Yoshida *et al.*<sup>3–6</sup> found the anomalous matching effect of the triangular microhole lattices on Al sheet. If the width of the Al film between holes is small, this system can be viewed as a superconducting honeycomb network.

Theoretical studies of superconducting networks began with de Gennes’ work<sup>7</sup> on the superconducting lasso, which is a ring with an arm attached to it, under the magnetic field. Subsequent work of Alexander<sup>8</sup> generalized de Gennes’ method, which is an application of the linearized Ginzburg-Landau equation, to the general superconducting networks. The equation that is derived by Alexander is called as de Gennes–Alexander network equation (dGA). Several works on ladder networks,<sup>9</sup> networks with an external source,<sup>10</sup> and  $n$  strips<sup>11</sup> were followed.<sup>12</sup>

Experiment on the regular superconducting lattice has been done on square lattices,<sup>13</sup>  $T_3$  lattices,<sup>14</sup> Kagomé lattices,<sup>15</sup> and honeycomb lattices.<sup>16,17</sup> There was also an experiment on disordered lattices.<sup>18</sup>

Previous theoretical studies were mainly done on the periodic systems, but recently experiment on the small micrometer-sized network ( $2 \times 2$  antidot cluster) has been done.<sup>19</sup> The transition temperature of this system is somewhat different from the periodic lattices. In the framework of the de Gennes–Alexander theory, they also calculated the transition temperature and the order-parameter distribution.

They found that the order parameter becomes zero at the center node when external magnetic field  $H_0$  satisfies  $H_0 a^2 / \Phi_0 \sim 0.5$ , where  $a$  is the lattice constant, and external flux dependence of the transition temperature agrees with the experiment qualitatively.<sup>19</sup> Therefore, it seems that there is a gap between the finite cluster and the periodic systems.

In this paper, we study finite superconducting networks with edge. Solving the de Gennes–Alexander network equation, we calculate the transition temperature, the order parameter distribution, and the distribution of the quantized fluxoid. We discuss the difference between the periodic lattices and the finite clusters. We show that the superconducting state of the finite clusters under the magnetic field becomes inhomogeneous and the order parameter at the interior bonds almost vanishes. Also we show that because of this property the transition temperature of the finite clusters is not much suppressed by the magnetic field, compared with periodic infinite lattices.

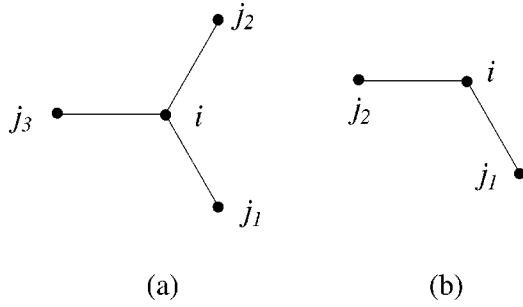
This paper is organized as follows. In Sec. II we give the details of our calculation and show the result of the honeycomb lattices. In Sec. III, we show the results of square lattices. Section IV is devoted to summary and discussion.

**II. HONEYCOMB NETWORKS**

In this section, we explain the methods of our calculation applied to superconducting networks in the  $x$ - $y$  plane under perpendicular magnetic field  $\mathbf{H} = (0, 0, H_0)$ . In the following, we consider two-dimensional flat networks that are composed of straight wires with same length  $a$ . Generally, the de Gennes–Alexander equation for the superconducting network is given as,<sup>8,12</sup>

$$\sum_j \Delta_j \exp(i\gamma_{i,j}) = n_i \Delta_i \cos \frac{a}{\xi}, \quad (1)$$

where the sum of  $j$  is taken over the nodes connected by wires with node  $i$ ,  $n_i$  is the number of wires connecting with node  $i$ , and  $\Delta_i$  denotes order parameter at node  $i$ . The phase  $\gamma_{i,j}$  is given as

FIG. 1. A lattice point  $i$  and its connected points  $j$ 's.

$$\gamma_{i,j} = \frac{2\pi}{\Phi_0} \int_i^j \mathbf{A} \cdot d\mathbf{s}. \quad (2)$$

In this section we use Landau gauge, and the vector potential is expressed as  $\mathbf{A} = (0, H_0 x, 0)$ . The line integral is over the contour along the wire. The temperature  $T$  dependence of the Landau-Ginzburg coherence length  $\xi$  near the zero-field transition temperature  $T_{C0}$  can be written as  $\xi = \xi_0 / \sqrt{1 - T/T_{C0}}$ , where  $\xi_0$  is the coherence length at zero temperature. For example, the de Gennes–Alexander network equation for the node  $i$  in Fig. 1(a) is given as

$$\sum_{j=1}^3 \Delta_j \exp(i \gamma_{i,j}) = 3 \Delta_i \cos \frac{a}{\xi}, \quad (3)$$

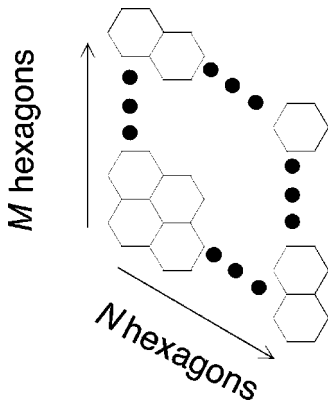
and for the node in Fig. 1(b),

$$\sum_{j=1}^2 \Delta_j \exp(i \gamma_{i,j}) = 2 \Delta_i \cos \frac{a}{\xi}. \quad (4)$$

We apply the above discussion to the honeycomb superconductive network (HSNW) as shown in Fig. 2 under magnetic field  $\mathbf{H} = (0, 0, H_0)$ . In the following discussion, we call the network shown in Fig. 2 as  $M \times N$  HSNW.

Lattice points of honeycomb networks are divided into two sublattices  $A$  and  $B$ . The coordinates of each lattice points in  $A$  and  $B$  sublattices are expressed as

$$\mathbf{r}^A(m, n) = \left( \frac{3}{2}n - \frac{1}{2}, \sqrt{3}m - \frac{\sqrt{3}}{2}n \right) a, \quad (5)$$

FIG. 2.  $M \times N$  honeycomb network.

$$\mathbf{r}^B(m, n) = \left( \frac{3}{2}n + \frac{1}{2}, \sqrt{3}m - \frac{\sqrt{3}}{2}n \right) a, \quad (6)$$

respectively. Here  $m$  and  $n$  are integers. For simplicity, order parameters at the lattice points  $\mathbf{r}^A(m, n)$  and  $\mathbf{r}^B(m, n)$  are written as  $\Delta^A(m, n)$  and  $\Delta^B(m, n)$ , respectively.

The applied magnetic flux per hexagon is  $\Phi = (3\sqrt{3}/2)a^2 H_0$ . The dGA equation at interior points  $\mathbf{r}^A(m, n)$  and  $\mathbf{r}^B(m, n)$  becomes

$$\begin{aligned} & \Delta^B(m, n) + e^{-(2\pi\Phi/\Phi_0)[(n/2)-(1/4)]} \Delta^B(m-1, n-1) \\ & + e^{(2\pi\Phi/\Phi_0)[(n/2)-(1/4)]} \Delta^B(m, n-1) \\ & = 3 \cos\left(\frac{a}{\xi}\right) \Delta^A(m, n), \end{aligned} \quad (7)$$

$$\begin{aligned} & \Delta^A(m, n) + e^{-(2\pi\Phi/\Phi_0)[(n/2)+(1/4)]} \Delta^A(m, n+1) \\ & + e^{(2\pi\Phi/\Phi_0)[(n/2)+(1/4)]} \Delta^A(m+1, n+1) \\ & = 3 \cos\left(\frac{a}{\xi}\right) \Delta^B(m, n). \end{aligned} \quad (8)$$

If  $\mathbf{r}$  is the edge point and the number of connected lattice points is two, which is the case shown in Fig. 1(b), dGA equation becomes the one similar to Eq. (4).

Divided by 2 or 3, these equations become eigenvalue equations with the eigenvalue  $\cos(a/\xi)$ . We solve it numerically, using a subroutine that contains transformation of general complex matrix to the Hessenberg matrix and the QR algorithm. Then, we can determine the transition temperature from its largest eigenvalue  $\cos(a/\xi) = \cos[(a\sqrt{1-T/T_{C0}})/\xi_0]$ .

The behavior of the superconducting transition temperature  $T_C$  under the magnetic field is shown in Fig. 3. The transition temperature of HSNW with periodic boundary condition shows dip structures at  $\Phi/\Phi_0 = \frac{1}{3}, \frac{2}{5}, \frac{3}{7}, \frac{1}{2}, \frac{3}{5}, \frac{4}{7}, \frac{3}{5}$ .

On the other hand, in  $M \times N$  HSNW with edge, we cannot find these structures. It should be also noted that decrease of transition temperature due to the applied magnetic field is smaller than that in the network with the periodic boundary condition. The difference of transition temperature between HSNW with periodic boundary condition and HSNW with edge can be explained as follows. The amplitude of order parameter in HSNW with edge decreases exponentially from edge point to center point at the transition temperature. The ‘‘bulk part’’ in the center of HSNW with edge has already changed to normal phase in the lower temperature than transition temperature of HSNW with edge. The transition temperature of network with edge is higher than that of the bulk part that corresponds the network with periodic boundary condition. In Fig. 4, amplitude of the order parameter as a function of distance from the edge point is shown for several values of the external field.

The distribution of fluxoid is determined from the phase of order parameter. If  $\xi > (\pi/2)a$ , the phase difference between lattice points  $\mathbf{r}_i$  and  $\mathbf{r}_j$  can be calculated as

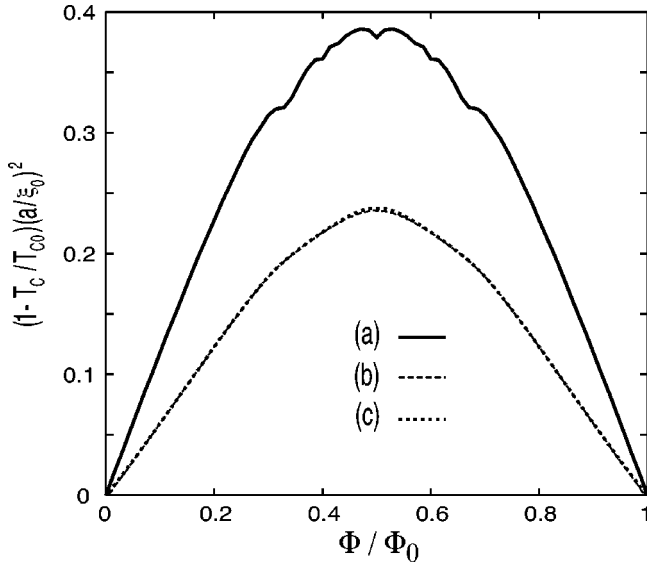


FIG. 3. The magnetic-field dependence of transition temperature of honeycomb superconducting networks (HSNW). (a) HSNW with periodic boundary condition, (b)  $10 \times 10$  HSNW, and (c)  $20 \times 20$  HSNW.

$$\phi_{i,j} = \arg\left(\frac{\Delta(j)e^{i\gamma_{i,j}}}{\Delta(i)}\right) - \gamma_{i,j}, \quad (9)$$

where the symbol  $\arg(z)$  denotes the principal value of the argument of complex number  $z$ , i.e.,  $-\pi < \arg(z) \leq \pi$ . For an arbitrary loop  $C$  in the network, the number of quantized fluxoids (the phase winding number),  $m(C)$ , passing through the loop  $C$  is

$$m(C) = -\frac{1}{2\pi} \sum_{C \langle i,j \rangle} \phi_{i,j}. \quad (10)$$

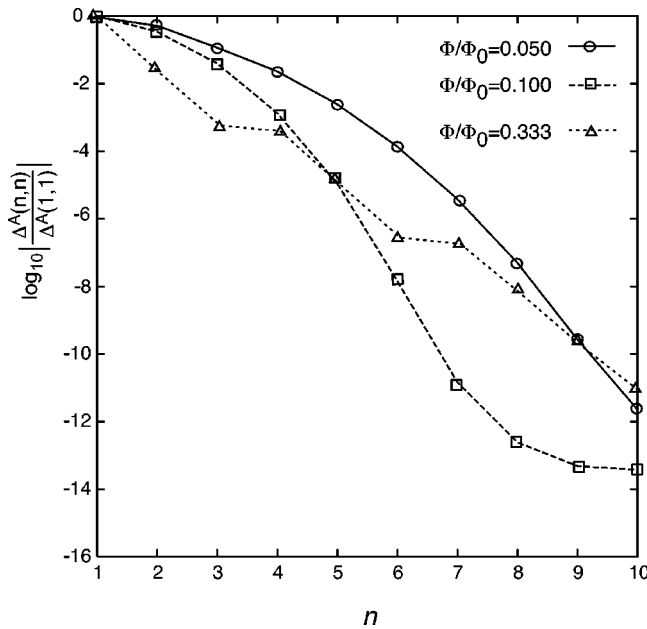


FIG. 4. Variations of amplitudes of order parameters of  $20 \times 20$  HSNW at the transition temperatures from the corner  $|\Delta^A(1,1)|$  to the center  $|\Delta^A(10,10)|$ .

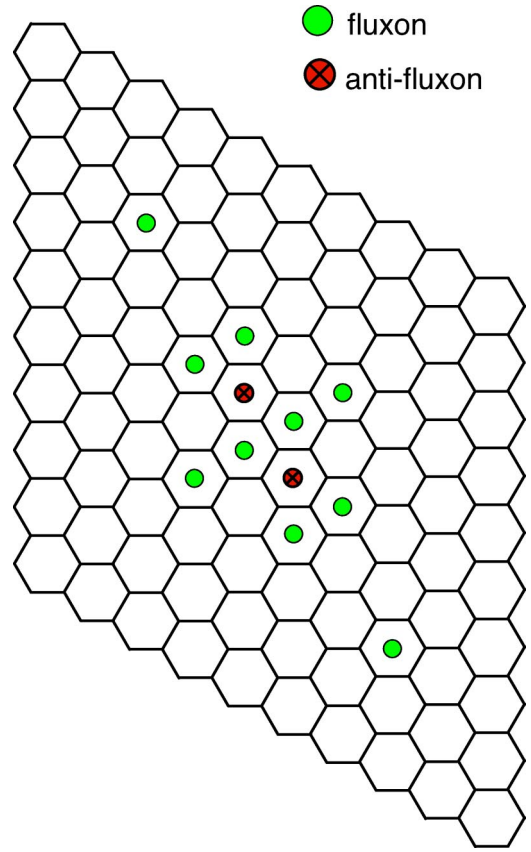


FIG. 5. (Color-online) Fluxon distribution of  $10 \times 10$  HSNW at  $\Phi / \Phi_0 = 0.100$ . A circle shows a single fluxon and  $\otimes$  shows an antifluxon.

Hereafter, we call the quantized fluxoid as a fluxon. Figures 5 and 6 show distributions of fluxon for HSNW with edge under the external magnetic field. For weak magnetic field, fluxons tend to locate in the center of the network. For increasing applied field, fluxons tend to form straight lines and line up along the network edge.

In Figs. 5 and 6, we can see antifluxons, which are surrounded by ordinary fluxons. By antifluxon we mean a fluxon whose direction is antiparallel to the external magnetic field. The appearance of the antifluxon can be understood as follows: if numbers of ordinary fluxons surround a single hexagon, then current flows around the center hexagon, which makes the magnetic field antiparallel. Fluxons appear according to the symmetry of the system, and when external field is not strong for such configuration of fluxons, it is sometimes energetically favorable to keep such configuration that makes the antifluxon.

In some cases, superconducting order is broken at the point in the wire that connects between two lattice nodes. For example, in Fig. 6, superconducting order is broken at the wire that locates the center of the network and an antifluxon passes through it.

### III. SQUARE LATTICE NETWORKS

In this section, we consider the square lattice with size  $2La \times 2La$ , where  $a$  is the length of the wire. We denote the

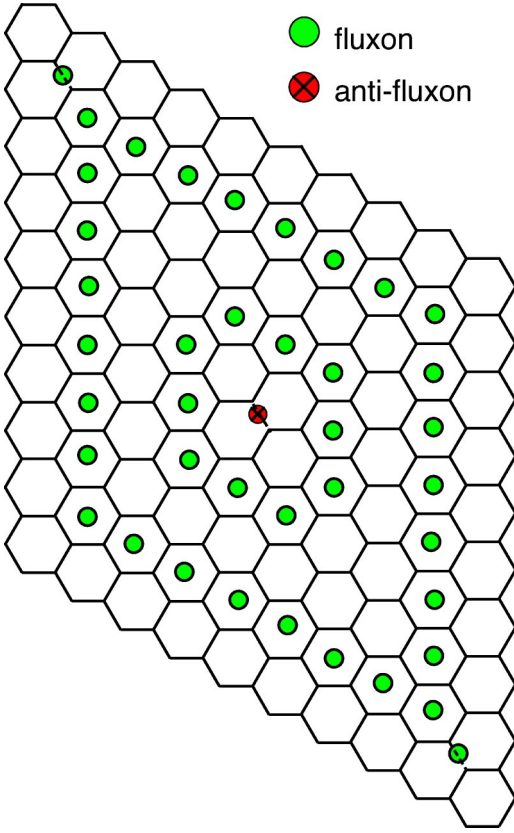


FIG. 6. (Color-online) Fluxon distribution of  $10 \times 10$  HSNW at  $\Phi/\Phi_0=0.400$ . Broken line shows that superconductivity of the bond is broken. Other symbols are same as Fig. 5.

lattice points as  $(na, ma)$ , where  $n$  and  $m$  are integers and  $-L \geq n$  and  $m \geq L$ . The de Gennes–Alexander network equation (1) for the square network is given by

$$\begin{aligned} & \Delta(n, m+1)e^{in\pi\phi} + \Delta(n, m-1)e^{-in\pi\phi} \\ & + \Delta(n+1, m)e^{-im\pi\phi} + \Delta(n-1, m)e^{im\pi\phi} \\ & = 4 \cos\left(\frac{a}{\xi}\right) \Delta(n, m), \end{aligned} \quad (11)$$

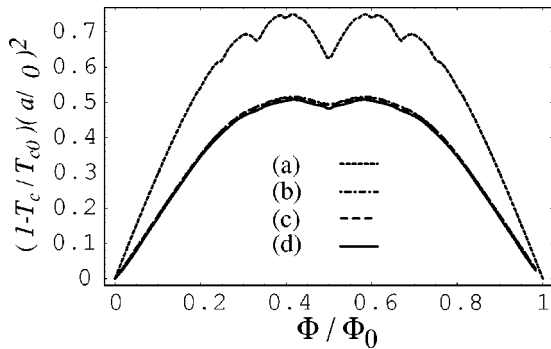


FIG. 7. Magnetic-field dependence of  $T_c$  of square superconducting lattices. (a) is for the periodic lattice, (b) for a lattice with size  $40 \times 40$ , (c) for  $20 \times 20$ , and (d) for  $10 \times 10$ .

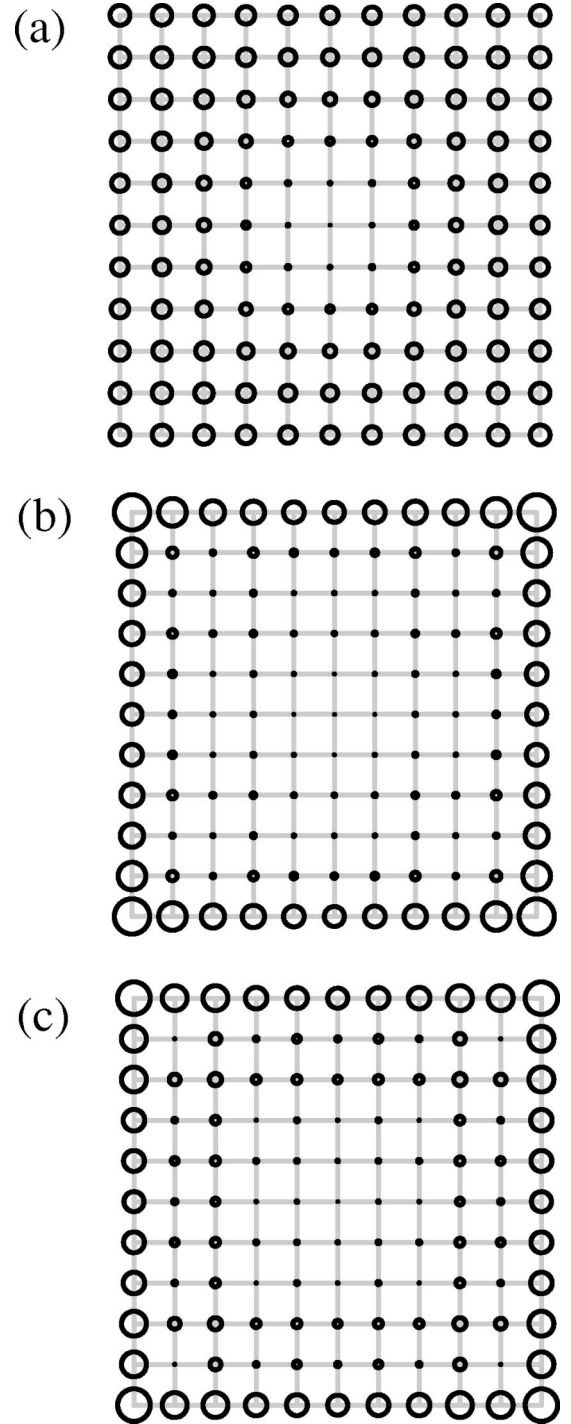


FIG. 8. Spatial distribution of the amplitude of the order parameter  $\Delta$  at nodes for  $\Phi/\Phi_0=0.033$  (a),  $\Phi/\Phi_0=0.333$  (b), and  $\Phi/\Phi_0=0.4833$  (c). Radius of the circle at each vortex shows relative magnitude of the order parameter  $|\Delta(n, m)|$  at the vertex.

where  $\Delta(n, m)$  is an order parameter at a lattice point  $(n, m)$ . Equation (11) is for the lattice points inside the network. For the lattice point at  $(n, L)$ , the dGA equation becomes

$$\begin{aligned} & \Delta(n, L-1)e^{-in\pi\phi} + \Delta(n+1, L)e^{-iL\pi\phi} + \Delta(n-1, L)e^{iL\pi\phi} \\ & = 3 \cos\left(\frac{a}{\xi}\right) \Delta(n, L). \end{aligned} \quad (12)$$

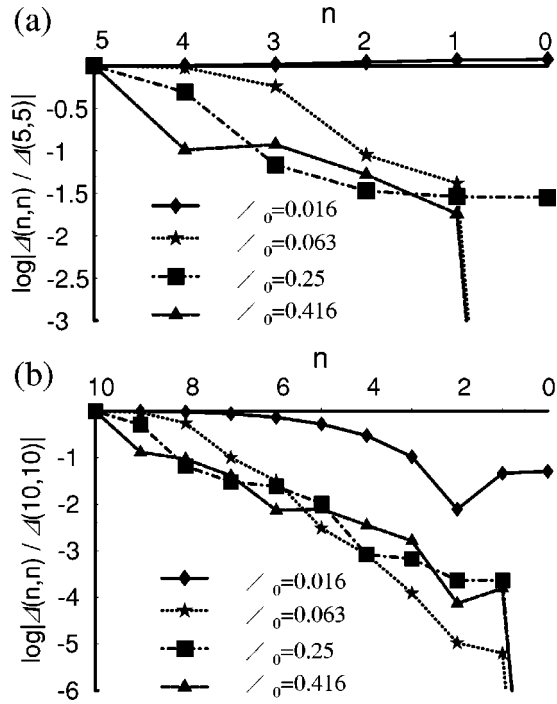


FIG. 9. Variation of the amplitude of the order parameter from the corner node to the center node along the diagonal line. (a)  $10 \times 10$  cluster; (b)  $20 \times 20$  cluster.

The equation for the other points at the edge of the lattice is similar. And for the point at  $(L,L)$ , the equation becomes

$$\Delta(L,L-1)e^{-iL\phi} + \Delta(L-1,L)e^{iL\phi} = 2 \cos\left(\frac{a}{\xi}\right) \Delta(L,L). \quad (13)$$

Also for the other corner points, similar equations hold.

We can solve the above equations as an eigenvalue problem in a manner similar to that for honeycomb networks. In Fig. 7, we show magnetic-field dependence of the transition temperature for the periodic lattice,  $10 \times 10$ ,  $20 \times 20$ , and  $40 \times 40$  lattices.

Similar to the honeycomb lattices, transition temperature for the lattice with the edge does not tend to that of the periodic lattice as the size of the lattice is increased.  $T_C$  of the periodic lattice shows several dips at  $\Phi/\Phi_0 = \frac{1}{2}, \frac{1}{3}, \frac{2}{3}, \frac{1}{4}, \frac{3}{4}, \dots$ . But  $T_C$  of finite clusters show only one dip at  $\Phi/\Phi_0 = \frac{1}{2}$ . This is because the superconducting state is bounded to the periphery of the lattice, as in the case of honeycomb lattices. For example, spatial dependence of the amplitude of the order parameter at each node is shown in Fig. 8 for  $10 \times 10$  lattice.

For weak external field, the order parameter does not change largely from the edge node to the center node. But for large field, the order parameter varies largely. We show the variation of magnitude of the order parameter in Fig. 9 for  $10 \times 10$  and  $20 \times 20$  lattices.

In these figures, the amplitude of the order parameter is normalized by the value at the corner node. Except very

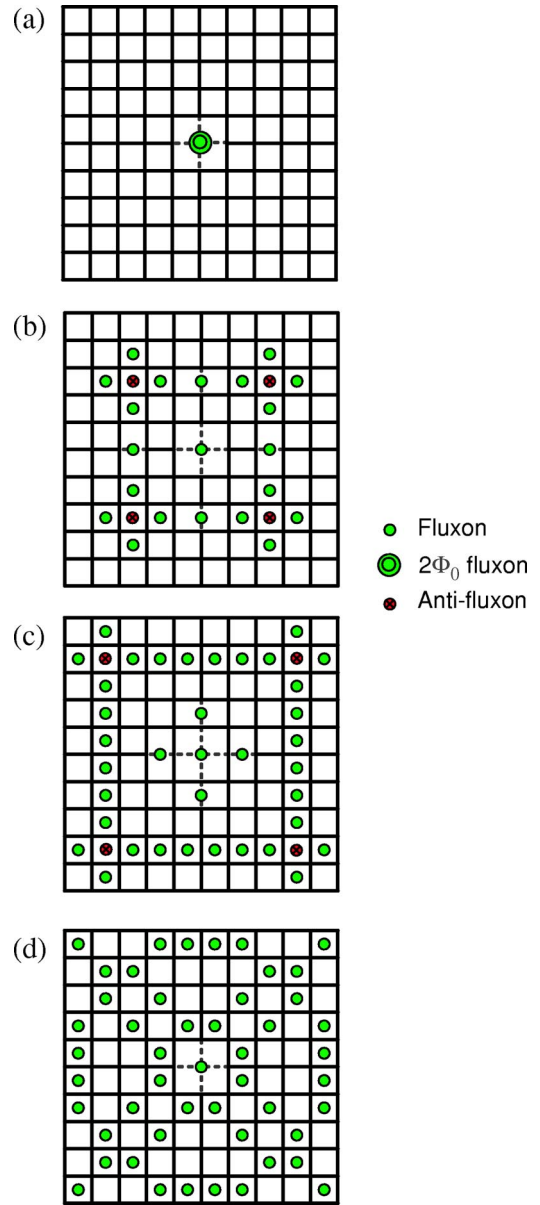


FIG. 10. (Color online) Spatial distribution of the quantized fluxoids for  $\Phi/\Phi_0=0.033$  (a),  $\Phi/\Phi_0=0.1833$  (b),  $\Phi/\Phi_0=0.333$  (c), and  $\Phi/\Phi_0=0.4833$  (d).  $\bigcirc$  shows  $2\Phi_0$  fluxon. Other symbols are the same as in Fig. 6.

small  $\Phi/\Phi_0$ , the amplitude decays exponentially with distance from the edge. Its decay rate becomes large for larger clusters.

We also calculate the phase winding number around each square, and deduce the distribution of fluxons. We show typical examples in Fig. 10. For weak field, the fluxoid enters from the center of the lattice. For some field value, the multi-quantum fluxon appears at the center, breaking the superconductivity of the surrounding wires, as shown in Fig. 10(a). In this case,  $2\Phi_0$  fluxon appears in the four squares around the center node, breaking superconductivity of four bonds. On increasing the field, fluxons move outward and sometimes an anti-fluxon appears, which is surrounded by ordinary fluxons, as shown in Fig. 10(b). On further increas-

ing the field, fluxons tend to form a line [Fig. 10(c)]. This is because the kinetic energy associated to the phase change of the order parameter becomes small, when the fluxons are aligned.

#### IV. SUMMARY AND CONCLUSION

In this paper, making use of the de Gennes–Alexander equation, we have investigated superconducting transition of honeycomb and square networks under the magnetic field. For both types of networks, transition temperatures of the finite clusters are not much decreased by the magnetic field, compared with periodic infinite lattice. It can be explained as follows: The order parameter of finite clusters becomes inhomogeneous under the magnetic field. At the edge the order parameter is large and decreases exponentially towards the center. Because the order parameter at interior bonds almost vanishes, transition temperature is determined mostly by the edge-bond superconductivity. Therefore the frustration at the interior bonds does not much suppress the transition temperature. Also system size dependence becomes weak.

The distribution of fluxons shows much variety of patterns. For strong magnetic field, fluxons tend to align along the edge. Ishida *et al.* observed fluxoid distribution on trian-

gular micro-hole lattice by the superconducting quantum interference device (SQUID) microscope and reported that magnetic fluxes form parallel lines.<sup>4</sup> Our calculations are consistent with their results. In addition, antifluxon appears associated with fluxons, similar to the mesoscopic superconducting square plates that were studied by Chibotaru *et al.*<sup>20</sup> Multiple fluxon also appears by breaking the superconductivity of surrounding bonds. These results may be verified by the SQUID microscope.

Our approach is applicable only at the phase-transition temperature. Therefore distribution of the order parameter and fluxons may change on decreasing the temperature below  $T_c$ . In order to study temperature dependence, we must solve full nonlinear Ginzburg-Landau equation. This is a future problem.<sup>21</sup>

#### ACKNOWLEDGMENTS

The authors would like to thank T. Ishida, M. Yoshida, and S. Nakata for discussions about their experiments. Also one of the authors (M.K.) would like to thank Y. Kayanuma and members of quantum physics research group of the Osaka Prefecture University for useful discussions.

\*Electronic address; gpsato@las.osaka-pct.ac.jp

†Electronic address: kato@ms.osakafu-u.ac.jp

<sup>1</sup>W.A. Little and R.D. Parks, Phys. Rev. Lett. **9**, 9 (1962).

<sup>2</sup>R.D. Parks and W.A. Little, Phys. Rev. **133**, A97 (1964).

<sup>3</sup>M. Yoshida, T. Ishida, and K. Okuda, Physica C **357-360**, 608 (2001).

<sup>4</sup>T. Ishida, M. Yoshida, K. Okuda, S.O.M. Sasase, K. Hojou, A. Odawara, A. Nagata, T. Morooka, S. Nakayama, and K. Chino, Physica C **357-360**, 604 (2001).

<sup>5</sup>M. Yoshida, S. Nakata, and T. Ishida, Supercond. Sci. Technol. **14**, 1166 (2001).

<sup>6</sup>T. Ishida, M. Yoshida, S. Okayasu, and K. Hojou, Supercond. Sci. Technol. **14**, 1128 (2001).

<sup>7</sup>P.G. de Gennes, C. R. Acad. Sc. Paris Ser. II **292**, 279 (1981).

<sup>8</sup>S. Alexander, Phys. Rev. B **27**, 1541 (1983).

<sup>9</sup>J. Simonin, D. Rodrigues, and A. López, Phys. Rev. Lett. **49**, 944 (1982).

<sup>10</sup>H.J. Fink, A. López, and R. Maynard, Phys. Rev. B **26**, 5237 (1982).

<sup>11</sup>R. Rammal, T.C. Lubensky, and G. Toulouse, Phys. Rev. B **27**,

2820 (1983).

<sup>12</sup>*Connectivity and Superconductivity*, edited by J. Berger and J. Rubinstein (Springer, Berlin, 2000).

<sup>13</sup>B. Pannetier, J. Chaussy, and R. Rammal, Phys. Rev. Lett. **53**, 845 (1984).

<sup>14</sup>C.C. Abilio, P. Butaud, T. Fournier, and B. Pannetier, Phys. Rev. Lett. **83**, 5102 (1999).

<sup>15</sup>M.J. Higgins, Y. Xiao, S. Bhattacharya, P.M. Chaikin, S. Sethuraman, R. Bojko, and D. Spencer, Phys. Rev. B **61**, R894 (2000).

<sup>16</sup>Y. Xiao, D.A. Huse, P.M. Chaikin, M.J. Higgins, S. Bhattacharya, and D. Spencer, Phys. Rev. B **65**, 214503 (2002).

<sup>17</sup>B. Pannetier, J. Chaussy, and R. Rammal, Jpn. J. Appl. Phys., Suppl. **26**, 1994 (1987).

<sup>18</sup>C. Bonetto, N.E. Israeloff, N. Pokrovskiy, and R. Bojko, Phys. Rev. B **58**, 128 (1998).

<sup>19</sup>T. Puig, E. Rosseel, L.V. Look, M.J.V. Bael, V.V. Moshchalkov, and Y. Bruynseraede, Phys. Rev. B **58**, 5744 (1998).

<sup>20</sup>V.B.L.F. Chibotaru, A. Ceulemans, and V.V. Moshchalkov, Nature (London) **408**, 833 (2000).

<sup>21</sup>M. Ako and M. Kato (unpublished).